ResearchGate

See discussions, stats, and author profiles for this publication at: https://www.researchgate.net/publication/267326617

Dissociation Pathways of Benzylpyridinium "Thermometer" Ions Depend on the Activation Regime: An IRMPD Spectroscopy Study

ARTICLE *in* JOURNAL OF PHYSICAL CHEMISTRY LETTERS · NOVEMBER 2014

Impact Factor: 7.46 · DOI: 10.1021/jz501903b

CITATION
1

READS
41

5 AUTHORS, INCLUDING:

Denis Morsa
University of Liège
5 PUBLICATIONS **51** CITATIONS
SEE PROFILE

Valérie Gabelica
French Institute of Health and Medical Resea…
117 PUBLICATIONS **3,138** CITATIONS
SEE PROFILE

Edwin De Pauw
University of Liège
383 PUBLICATIONS **7,232** CITATIONS
SEE PROFILE

Available from: Denis Morsa
Retrieved on: 30 January 2016

THE JOURNAL OF PHYSICAL CHEMISTRY Letters

Letter

pubs.acs.org/JPCL

Dissociation Pathways of Benzylpyridinium "Thermometer" Ions Depend on the Activation Regime: An IRMPD Spectroscopy Study

Denis Morsa,[†] Valérie Gabelica,[†,∥] Frédéric Rosu,[†,⊥] Jos Oomens,[‡,§] and Edwin De Pauw*[,†]

[†]Mass Spectrometry Laboratory, University of Liege, B6c Sart-Tilman, B-4000 Liege, Belgium

[‡]Radboud University, Institute for Molecules and Materials, FELIX Laboratory, Toernooiveld 7, 6525ED Nijmegen, The Netherlands

[§]Van't Hoff Institute for Molecular Sciences, University of Amsterdam, Science Park 904, 1098 XH Amsterdam, The Netherlands

Supporting Information

ABSTRACT: The dissociation of benzylpyridinium "thermometer" ions is widely used to calibrate the internal energy of ions produced in mass spectrometry. The fragmentation mechanism is usually believed to yield a benzylium cation, although recent studies suggest the possibility of a rearrangement leading to the tropylium isomer, which would compromise the accuracy of energy calibrations. In this study, we used IRMPD spectroscopy to probe the dissociation pathways of the *p*-(*tert*-butyl)-benzylpyridinium ion. Our results show that the formation of both benzylium and tropylium products is feasible depending on the activation regime and on the reaction time scale. Varying the trapping delays in the hexapole gives insight into a rearrangement mechanism occurring through consecutive reactions with an isomerization from benzylium to tropylium. Our work provides experimental validations for the established calibration procedure and highlights the adequacy of IRMPD spectroscopy to qualitatively resolve gas-phase rearrangement kinetics.

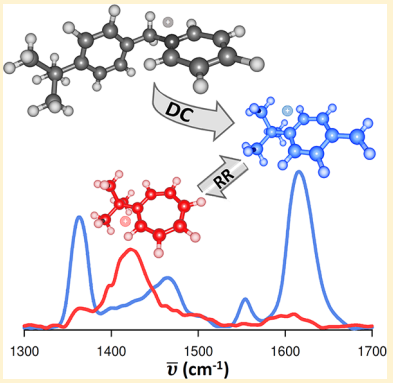

SECTION: Spectroscopy, Photochemistry, and Excited States

The internal energy distribution of a population of ions drastically influences its reactivity and affects its physicochemical properties. The control of the ion internal energy is therefore of crucial importance for mass spectrometry applications, especially for structural elucidations or for the analysis of fragile assemblies like noncovalent complexes.[1,2] In this context, the dissociation of "thermometer" ions allows one to evaluate the ion heating inside a mass spectrometer, especially during the ionization process.[3] The thermometer ions are designed to undergo a specific fragmentation when their internal energy exceeds a critical threshold E_0. The measured survival yield of the precursor ion SY = $I_P/(I_P + \sum I_{frag})$ is therefore equal to the fraction of ions having an internal energy below E_0 and is indicative of the internal energy distribution. Among the different "thermometer" ions that have been reported in the literature,[4,5] substituted benzylpyridinium ions have become the most popular to investigate the internal energy of ions produced using well-established soft ionization methods[6−11] and remain widespread in many recent studies.[12−17]

In the early work, the fragmentation mechanism of benzylpyridinium ions (**BzPy**) was assumed to occur through a direct bond cleavage (DC), consisting of the loss of a neutral pyridine and the formation of the corresponding benzylium cation (**Bz**) (Scheme 1). Assuming that this reaction goes through a loose transition state (TS), the reverse activation barrier could be neglected[18] and the critical fragmentation threshold E_0 was calculated as the zero point energy difference between the products and the reactant. However, in 2009, Zins et al. reported the concomitant formation of the tropylium isomer (**Tr**) for several benzylpyridinium ions (Scheme 1) on the basis of experimental evidence arising from kinetic energy release (KER) measurements[19] and gas-phase reactivity experiments.[20,21] Following theoretical calculations, they imparted the formation of **Tr** to a distinct reaction pathway involving a four-step rearrangement process (RR) occurring prior to dissociation of the neutral pyridine.[19] Because this alternative pathway could compromise the reliability of previous internal energy calibrations,[19,20] further investigations are required to both confirm the presence of **Tr** and identify its formation mechanism.

Scheme 1. Structure of a Substituted Benzylpyridinium Cation (BzPy) and of the Corresponding Benzylium Cation (Bz) and Tropylium Cation (Tr)

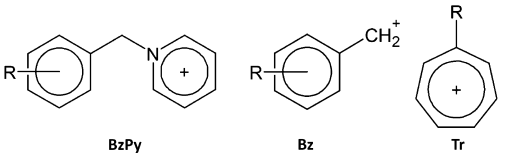

Here we explored a wide range of activation conditions resulting in the loss of the neutral pyridine under slow heating conditions and interrogated the structure of the resulting

Received: September 8, 2014
Accepted: October 16, 2014

 © XXXX American Chemical Society dx.doi.org/10.1021/jz501903b | *J. Phys. Chem. Lett.* 2014, 5, 3787−3791

fragment using infrared multiple photon dissociation (IRMPD) spectroscopy.[22−24] To this end, *p*-(*tert*-butyl) substituted benzylpyridinium ions (m/z = 226) were electrosprayed, transferred through a sampling cone where they can be activated, and accumulated in a hexapole ion trap for 1 to 9 s. Depending on the hexapole trapping time and trapping voltages, further dissociation or rearrangement of ions could take place. The generated ion population was then stored in the cell of a Fourier transform-based mass analyzer (FT-ICR), where the $C_{11}H_{15}^+$ fragment ion corresponding to neutral pyridine loss (m/z = 147) was isolated and exposed to IR photons originating from the tunable free electron laser (FEL) at the FELIX user facility.[25,26]

The IRMPD spectra of the *p*-(*tert*-butyl) substituted fragment ions $C_{11}H_{15}^+$ (m/z = 147) generated using sampling cone voltages of 60 and 100 V are, respectively, represented by the blue and red traces in Figure 1a. They are obtained by

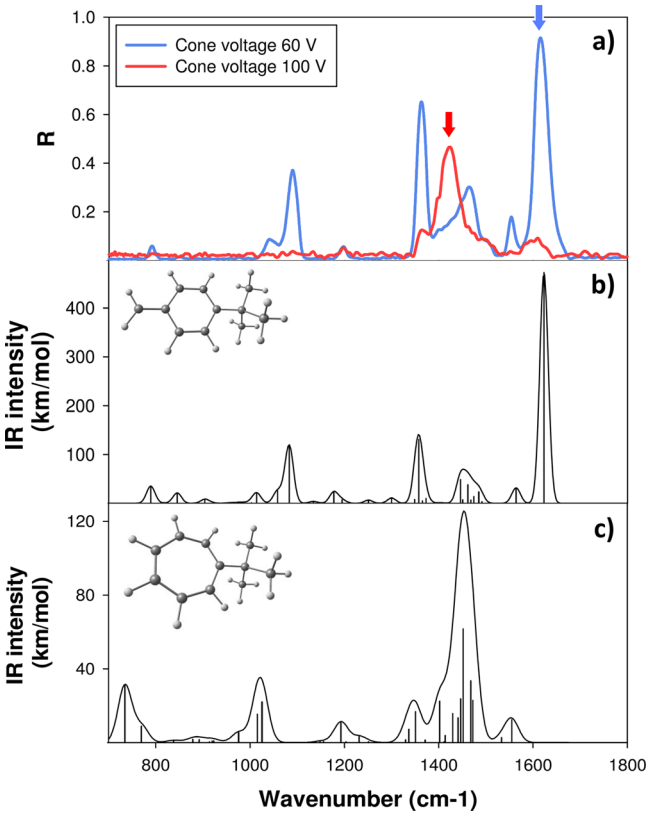

Figure 1. (a) Experimental IRMPD spectra of *p*-(*tert*-butyl) substituted fragment ions $C_{11}H_{15}^+$ obtained using soft (blue trace) and harsh (red trace) source cone voltage conditions (hexapole axial trapping voltage = 39.5 V, hexapole accumulation time = 9 s). (b) Computed IR spectrum of the *p*-(*tert*-butyl)benzylium cation. (c) Computed IR spectrum of the *p*-(*tert*-butyl)tropylium cation.

monitoring the IRMPD fragmentation yield, *R*, defined by eq 1, as a function of the photon wavenumber $\bar{\nu}$.

$$R = \frac{\sum I_{IR\_frag}}{(I_{C_{11}H_{15}^+} + \sum I_{IR\_frag})} \quad (1)$$

where $\sum I_{IR\_frag}$ is the total intensity of the radiation-induced fragments and $I_{C_{11}H_{15}}$+ is the intensity of the $C_{11}H_{15}^+$ ion.

The two IRMPD spectra are strikingly different, despite similar radiation-induced fragmentation channels corresponding to losses of CH_3 (m/z = 132), C_2H_4 (m/z = 119), and C_3H_6 (m/z = 105) (Supporting Information, Figure S-1). The fragments generated upon softer source conditions (low sampling cone voltage) display six major absorption bands at 1040, 1090, 1360, 1465, 1550, and 1615 cm^{-1}, which agree with the predicted bands of the *p*-(*tert*-butyl)benzylium cation (Figure 1b) and with previous results of Zins et al. (IRMPD performed in a quadrupole ion trap at the CLIO facility[21]). The fragments generated upon harsher source conditions absorb at 1360, 1425, and 1600 cm^{-1}, matching the theoretical spectrum of the *p*-(*tert*-butyl)tropylium cation (Figure 1c).

These results suggest that the dissociation of benzylpyridinium ions either leads to **Bz** or to **Tr** depending on the activation regime. At low internal energy content, only the reactions characterized by low activation energies are sampled. Under such conditions, **Bz** is highly favored, which reflects the fact that the formation of the associated loose TS is both enthalpically and entropically favored compared with the tight TSs likely formed during structural rearrangements leading to **Tr**.[19,20,27] However, an increase in the internal energy, which allows exploration of reaction channels characterized by higher activation energies, greatly promotes the formation of **Tr**. This observation could be imparted to subsequent isomerization of **Bz**, leading to an equilibrium mixture highly favoring the thermodynamically more stable **Tr**.[28] This increased stability is supported by our calculations that reveal that the *p*-(*tert*-butyl)tropylium cation is 0.18 eV more stable than its benzylium isomer.

Of interest for the energy calibration procedure based on thermometer ions is to determine whether the majority of isomerization occurs prior to or after dissociation of the pyridine, as both pathways seem conceivable a priori.[29−31] To this end, we estimated the relative abundances of **Bz** and **Tr** isomers of the $C_{11}H_{15}^+$ ion formed under different conditions. To avoid systematic recording of the entire IRMPD spectra, we monitored the IRMPD fragmentation yields *R* at two different laser frequencies: 1613 (λ = 6.2 μm) and 1428 cm^{-1} (λ = 7.0 μm). The values are represented as a bar chart in Figure 2. The two selected wavelengths are indicated by arrows in Figure 1 and correspond to the most intense absorption bands of the benzylium and tropylium cations, respectively. They are associated with ring deformations as well as with a stretching of the $C_{aromatic}-C_{benzylic}$ bond for the benzylium ion.[32,33] It should be noted that because the maximum absorption intensities are different for both cations the relative fragmentation yields do not quantitatively reflect the relative populations. Moreover, at the selected frequencies, the fragmentation intensity of the alternative isomer is not completely zero, so some "cross talk" is expected to be present in the relative abundances presented in Figure 2. For each activation condition, we also report the fragmentation yield *R* of the initially sprayed *p*-(*tert*-butyl)benzylpyridinium ions (m/z = 226) as a witness of the ion activation regime (black curve).

We first focused on energetic aspects and monitored, for a 9 s accumulation time in the hexapole, the effect of the source sampling cone voltage (Figure 2a) and of the hexapole axial trapping voltage (Figure 2b) on the $C_{11}H_{15}^+$ ion population. In both cases, increasing the voltages leads to a decrease of *R* measured at 1613 cm^{-1} and a concomitant increase in *R* measured at 1428 cm^{-1}. In agreement with Figure 1, these observations suggest a population shift from mainly **Bz** to mainly **Tr** as the activation regime gets harsher.

dx.doi.org/10.1021/jz501903b | J. Phys. Chem. Lett. 2014, 5, 3787−3791

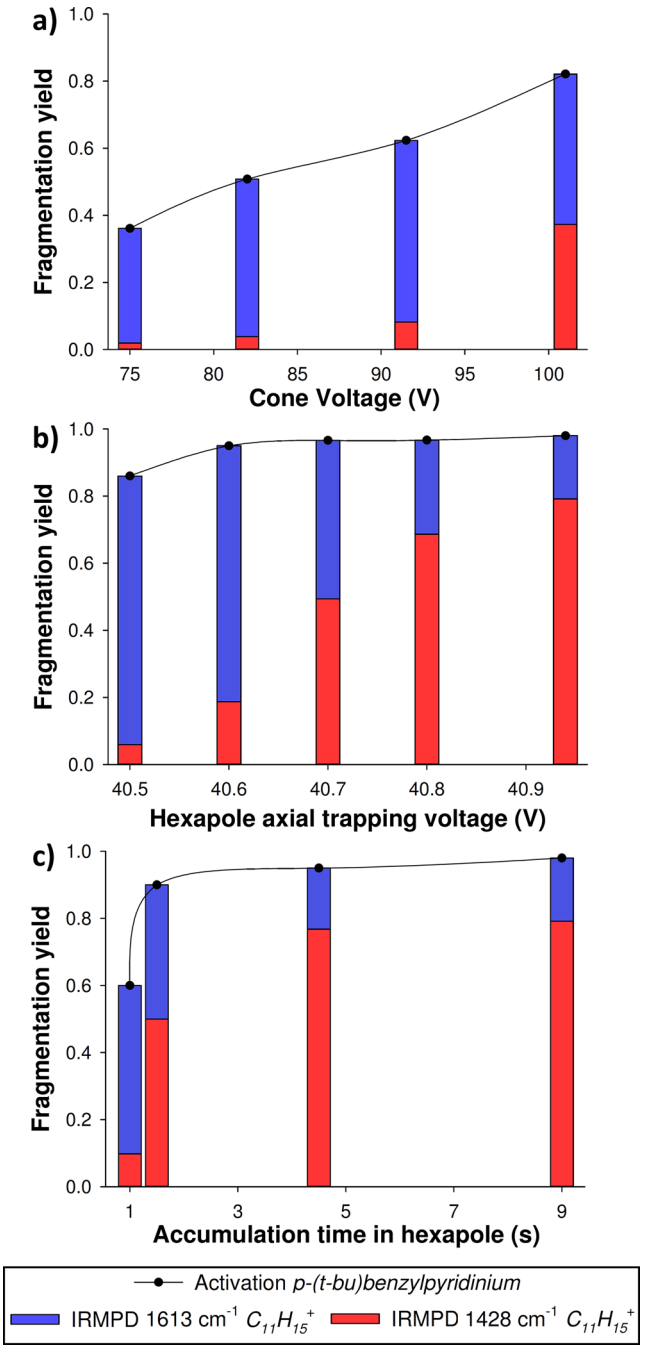

Figure 2. Influence of the activation regime on the structure of the $C_{11}H_{15}^+$ ion. The black curve corresponds to the total fragmentation yield R of the *p*-(*tert*-butyl)benzylpyridinium ion, and the bar chart reports the relative IRMPD fragmentation yield measured at 1613 and at 1428 cm^{-1}. (a) Influence of the sampling cone voltage (hexapole axial trapping voltage = 39.5 V, hexapole accumulation time = 9 s). (b) Influence of the hexapole axial trapping voltage (sampling cone voltage = 60 V, hexapole accumulation time = 9 s). (c) Influence of the accumulation time in the hexapole (sampling cone voltage = 60 V, hexapole axial trapping voltage = 40.94 V).

We then investigated the influence of the reaction time scale, monitoring the IRMPD fragmentation yield R as a function of the accumulation time in the hexapole (Figure 2c). The sampling cone and the hexapole axial trapping voltages were, respectively, set to 60 and 40.94 V, which corresponded to favorable conditions to form **Tr** for long (9 s) trapping delays. (See Figure 2b.) Figure 2c shows that for hexapole accumulation times of 1 s or shorter, the IRMPD fragmentation of $C_{11}H_{15}^+$ remains highly efficient at 1613 cm^{-1} and therefore **Bz** is the major dissociation product. However, when the accumulation time is increased to more than one second, the fragmentation yield measured at 1428 cm^{-1} gradually increases and the $C_{11}H_{15}^+$ ion becomes predominantly **Tr**. As the population of surviving *p*-(*tert*-butyl)benzylpyridinium ions is already below 10% of the total ion population after 1.5 s of trapping time, the formation of **Tr** can only be attributed to a gradual isomerization of **Bz** upon additional slow-heating activation provided by increasing numbers of collisions. These results thus suggest that most of **Tr** population is formed after the pyridine loss. The reaction time-scale effect (seconds on the FELIX ESI-FTICR setup) may explain why **Tr** was not observed in a previous IRMPD study performed at CLIO, where the total trapping time was set to 0.4 s.[21]

In conclusion, our results demonstrate that both **Bz** and **Tr** can be formed after dissociation of the *p*-(*tert*-butyl)-benzylpyridinium ion and that their relative abundances depend on the activation regime. Under our slow-heating conditions, the breaking of the C−N bond systematically takes place first and leads to **Bz** according to a direct cleavage pathway. The formation of **Tr** seems to occur in a second step by subsequent isomerization of **Bz** provided that sufficient energy inputs and reaction times (over seconds) are available. An outline of the potential energy surface accounting for these observation is given in the Supporting Information (Figure S-2). In contrast with the mechanism proposed by Zins et al.[19] after experiments on metastable ions under high-energy conditions, our results suggest that no competition between reaction pathways that could affect the reliability of the internal energy calibrations is involved. Even though we only investigated in depth the *p*-(*tert*-butyl)benzylpyridinium cation previously described as prone to generate tropylium,[20] alike IRMPD spectra were obtained for the *p*-(methyl)benzylpyridinium cation (Supporting Information, Figure S-3), and a similar behavior is expected for other thermometer ions. Consequently, in agreement with the original method applied for the majority of published data, only the loose TS leading to **Bz** has to be considered to calculate the critical energy threshold E_0 for dissociation of benzylpyridinium ions in the context of soft activation methods.

From an experimental point of view, we were able to firmly establish the formation of **Tr**, which was not observed in previous spectroscopic investigations.[21] This highlights the influence of storage times when preparing the ion population for irradiation and indicates how cautious one should be comparing and evaluating results obtained on different experimental platforms. Our work may also open new venues to qualitatively study gas-phase isomerization kinetics by IRMPD spectroscopy and by mass spectrometry in general.[34−36]

EXPERIMENTAL AND COMPUTATIONAL METHODS

The *p*-(*tert*-butyl)benzylpyridinium salt was synthesized by condensation of the *p*-(*tert*-butyl)benzyl chloride with pyridine. The recrystallized salt was solubilized with acetonitrile/water (50/50) and injected at 10^{-5} mol/L. The hexapole ion guide was operated at a DC bias of 38 V and was filled with N_2 at a pressure of 1.9×10^{-3} mbar. For ion storage, axial trapping voltages were applied to the entrance and exit lenses. The

dx.doi.org/10.1021/jz501903b | J. Phys. Chem. Lett. 2014, 5, 3787−3791

former was set to 41 V and the latter was varied between 40.4 and 40.94 V. Data were analyzed using SigmaPlot 12.5 software. The structure, energy, and harmonic frequencies of the *p*-(*tert*-butyl)benzylium and *p*-(*tert*-butyl)tropylium cations were determined at the B3LYP level using the 6-311++G(d,p) basis set in Gaussian 09. Reported total energy was corrected for zero-point vibrational energies, and the harmonic frequencies were scaled by 0.975 to generate theoretical IR spectra.[37]

■ ASSOCIATED CONTENT

Supporting Information

Mass spectra highlighting fragmentation channels consecutive to IRMPD irradiation, potential energy surface (PES) relative to the dissociation of the *p*-(*tert*-butyl)benzylpyridinium cation under slow-heating activation and IRMPD spectra of the *p*-(methyl)benzylpyridinium cation, as noted in the text. This material is available free of charge via the Internet at http://pubs.acs.org.

■ AUTHOR INFORMATION

Corresponding Author

*E-mail: e.depauw@ulg.ac.be.

Present Addresses

[‖]V.G.: U869 - ARNA Laboratory, Inserm & Univ. Bordeaux, F-33600 Pessac, France.

[⊥]F.R.: CNRS UMS 3033 & Inserm US001, IECB, Univ. Bordeaux, F-33600 Pessac, France.

Notes

The authors declare no competing financial interest.

■ ACKNOWLEDGMENTS

The research leading to these results has received funding from the European Community's Seventh Framework Programme (*FP7*/2007-2013) under grant agreement no. 226716. We thank the F.R.S.-FNRS for financial support and the FELIX staff for their skillful assistance.

■ REFERENCES

(1) Konijnenberg, A.; Butterer, A.; Sobott, F. Native Ion Mobility-Mass Spectrometry and Related Methods in Structural Biology. *Biochim. Biophys. Acta* **2013**, *1834*, 1239−56.

(2) Benesch, J. L.; Robinson, C. V. Mass Spectrometry of Macromolecular Assemblies: Preservation and Dissociation. *Curr. Opin. Struct. Biol.* **2006**, *16*, 245−51.

(3) Gabelica, V.; De Pauw, E. Internal Energy and Fragmentation of Ions Produced in Electrospray Sources. *Mass Spectrom. Rev.* **2005**, *24*, 566−87.

(4) Cooks, R. G.; Ast, T.; Kralj, B.; Kramer, V.; Zigon, D. Internal Energy Distributions Deposited in Doubly and Singly Charged Tungsten Hexa-Carbonyl Ions Generated by Charge Stripping, Electron Impact, And Charge Exchange. *J. Am. Soc. Mass Spectrom.* **1990**, *1*, 16−27.

(5) Voyksner, R. D.; Pack, T. Investigation of Collisional-Activation Decomposition Process and Spectra in the Transport Region of an Electrospray Single Quadrupole Mass Spectrometer. *Rapid Commun. Mass Spectrom.* **1991**, *5*, 263−268.

(6) Derwa, F.; De Pauw, E.; Natalis, P. New Basis for a Method for the Estimation of Secondary Ion Internal Energy Distribution in "Soft" Ionisation Techniques. *Org. Mass. Spectrom.* **1991**, *26*, 117−118.

(7) Derwa, F.; De Pauw, E. Evaluation of Internal Energy of Secondary Ions in LSIMS. *Spectrosc. Int. J.* **1989**, *7*, 227−232.

(8) Collette, C.; Pauw, E. D. Calibration of the Internal Energy Distribution of Ions Produced by Electrospray. *Rapid Commun. Mass Spectrom.* **1998**, *12*, 165−170.

(9) Gabelica, V.; De Pauw, E.; Karas, M. Influence of the Capillary Temperature and the Source Pressure on the Internal Energy Distribution of Electrosprayed Ions. *Int. J. Mass Spectrom.* **2004**, *231*, 189−195.

(10) Luo, G.; Marginean, I.; Vertes, A. Internal Energy of Ions Generated by Matrix-Assisted Laser Desorption/Ionization. *Anal. Chem.* **2002**, *74*, 6185−6190.

(11) Greisch, J. F.; Gabelica, V.; Remacle, F.; De Pauw, E. Thermometer Ions for Matrix-Enhanced Laser Desorption/Ionization Internal Energy Calibration. *Rapid Commun. Mass Spectrom.* **2003**, *17*, 1847−54.

(12) Tang, H.-W.; Ng, K.-M.; Lu, W.; Che, C.-M. Ion Desorption Efficiency and Internal Energy Transfer in Carbon-Based Surface-Assisted Laser Desorption/Ionization Mass Spectrometry: Desorption Mechanism(s) and the Design of SALDI Substrates. *Anal. Chem.* **2009**, *81*, 4720−4729.

(13) Huang, Y.; Yoon, S. H.; Heron, S. R.; Masselon, C. D.; Edgar, J. S.; Turecek, F.; Goodlett, D. R. Surface Acoustic Wave Nebulization Produces Ions with Lower Internal Energy than Electrospray Ionization. *J. Am. Soc. Mass Spectrom.* **2012**, *23*, 1062−70.

(14) DeBord, J. D.; Verkhoturov, S. V.; Perez, L. M.; North, S. W.; Hall, M. B.; Schweikert, E. A. Measuring the Internal Energies of Species Emitted from Hypervelocity Nanoprojectile Impacts on Surfaces Using Recalibrated Benzylpyridinium Probe Ions. *J. Chem. Phys.* **2013**, *138*, 214301.

(15) Flanigan, P. M. t.; Shi, F.; Perez, J. J.; Karki, S.; Pfeiffer, C.; Schafmeister, C.; Levis, R. J. Determination of Internal Energy Distributions of Laser Electrospray Mass Spectrometry Using Thermometer Ions and Other Biomolecules. *J. Am. Soc. Mass Spectrom.* **2014**, *25*, 1572−1582.

(16) Morsa, D.; Gabelica, V.; De Pauw, E. Effective Temperature of Ions in Traveling Wave Ion Mobility Spectrometry. *Anal. Chem.* **2011**, *83*, 5775−82.

(17) Hartmanova, L.; Frycak, P.; Soural, M.; Turecek, F.; Havlicek, V.; Lemr, K. Ion Internal Energy, Salt Tolerance and a New Technical Improvement of Desorption Nanoelectrospray. *J. Mass Spectrom.* **2014**, *49*, 750−4.

(18) Cook, R. G.; Beynon, J. H.; Caprioli, R. H.; Lester, G. R. *Metastable Ions*; Elsevier: Amsterdam, 1973.

(19) Zins, E.-L.; Pepe, C.; Rondeau, D.; Rochut, S.; Galland, N.; Tabet, J. C. Theoretical and Experimental Study of Tropylium Formation from Substituted Benzylpyridinium Species. *J. Mass Spectrom.* **2009**, *44*, 12−17.

(20) Zins, E.-L.; Rondeau, D.; Karoyan, P.; Fosse, C.; Rochut, S.; Pepe, C. Investigations of the Fragmentation Pathways of Benzylpyridinium Ions under ESI/MS Conditions. *J. Mass Spectrom.* **2009**, *44*, 1668−75.

(21) Zins, E.-L.; Pepe, C.; Schroder, D. Methylene-Transfer Reactions of Benzylium/Tropylium Ions with Neutral Toluene Studied by Means of Ion-Trap Mass Spectrometry. *Faraday Discuss.* **2010**, *145*, 157−169.

(22) Laskin, J.; Futrell, J. H. Activation of Large Ions in FT-ICR Mass Spectrometry. *Mass Spectrom. Rev.* **2005**, *24*, 135−67.

(23) Polfer, N. C.; Oomens, J. Reaction Products in Mass Spectrometry Elucidated with Infrared Spectroscopy. *Phys. Chem. Chem. Phys.* **2007**, *9*, 3804−17.

(24) Valle, J. J.; Eyler, J. R.; Oomens, J.; Moore, D. T.; van der Meer, A. F. G.; von Helden, G.; Meijer, G.; Hendrickson, C. L.; Marshall, A. G.; Blakney, G. T. Free Electron Laser-Fourier Transform Ion Cyclotron Resonance Mass Spectrometry Facility for Obtaining Infrared Multiphoton Dissociation Spectra of Gaseous Ions. *Rev. Sci. Instrum.* **2005**, *76*, 023103.

(25) Knippels, G.; Mols, R.; van der Meer, A.; Oepts, D.; van Amersfoort, P. Intense Far-Infrared Free-Electron Laser Pulses with a Length of Six Optical Cycles. *Phys. Rev. Lett.* **1995**, *75*, 1755−1758.

(26) Oepts, D.; Van Der Meer, A. F. G.; Van Amersfoort, P. W. The Free-Electron-Laser User Facility FELIX. *Infrared Phys. Technol.* **1995**, *36*, 297−308.
(27) McLafferty, F. W.; Winkler, J. Gaseous Tropylium, Benzyl, Tolyl, And Norbornadienyl Cations. *J. Am. Chem. Soc.* **1974**, *96*, 5182−5189.
(28) McLafferty, F. W.; Bockhoff, F. M. Formation of Benzyl and Tropylium Ions from Gaseous Toluene and Cycloheptatriene Cations. *J. Am. Chem. Soc.* **1979**, *101*, 1783−1786.
(29) Seo, J.; Kim, S. J.; Shin, S. K. Energy- And Time-Dependent Branching to Competing Paths in Coupled Unimolecular Dissociations of Chlorotoluene Radical Cations. *Bull. Korean Chem. Soc.* **2014**, *35*, 833−838.
(30) Shinly, S. K.; Han, S.-J.; Kim, B. Time-Resolved Photodissociation of p-Bromotoluene Ion As a Probe of Ion Internal Energy. *Int. J. Mass Spectrom. Ion Processes* **1996**, *157/158*, 345−355.
(31) Choe, J. C. Formation of $C_7H_7^+$ from Benzyl Chloride and Chlorotoluene Molecular Ions: A Theoretical Study. *J. Phys. Chem. A* **2008**, *112*, 6190−6197.
(32) Chiavarino, B.; Crestoni, M. E.; Dopfer, O.; Maitre, P.; Fornarini, S. Benzylium versus Tropylium Ion Dichotomy: Vibrational Spectroscopy of Gaseous C8H9+ Ions. *Angew. Chem., Int. Ed. Engl.* **2012**, *51*, 4947−9.
(33) Chiavarino, B.; Crestoni, M. E.; Fornarini, S.; Dopfer, O.; Lemaire, J.; Maître, P. IR Spectroscopic Features of Gaseous C7H7O+ Ions: Benzylium versus Tropylium Ion Structures. *J. Phys. Chem. A* **2006**, *110*, 9352−9360.
(34) Lagutschenkov, A.; Langer, J.; Berden, G.; Oomens, J.; Dopfer, O. Infrared Spectra of the Protonated Neurotransmitter Histamine: Competition between Imidazolium and Ammonium Isomers in the Gas Phase. *Phys. Chem. Chem. Phys.* **2011**, *13*, 15644−56.
(35) Zou, S.; Oomens, J.; Polfer, N. C. Competition between Diketopiperazine and Oxazolone Formation in Water Loss Products from Protonated ArgGly and GlyArg. *Int. J. Mass Spectrom.* **2012**, *316-318*, 12−17.
(36) Dey, A.; Fernando, R.; Abeysekera, C.; Homayoon, Z.; Bowman, J. M.; Suits, A. G. Photodissociation Dynamics of Nitromethane and Methyl Nitrite by Infrared Multiphoton Dissociation Imaging with Quasiclassical Trajectory Calculations: Signatures of the Roaming Pathway. *J. Chem. Phys.* **2014**, *140*, 054305.
(37) Andersson, M. P.; Uvdal, P. New Scale Factors for Harmonic Vibrational Frequencies Using the B3LYP Density Functional Method with the Triple-Basis Set 6-311+G(d,p). *J. Phys. Chem. A* **2005**, *109*, 2937−2941.